Amyloid Formation by Pro-Islet Amyloid Polypeptide Processing Intermediates: Examination of the Role of Protein Heparan Sulfate Interactions and Implications for Islet Amyloid Formation in Type 2 Diabetes†

Fanling Meng,‡ Andisheh Abedini,‡,§ Benben Song,‡ and Daniel P. Raleigh*,‡,||

Department of Chemistry, State University of New York at Stony Brook, Stony Brook, New York 11794-3400, and Graduate Program in Biochemistry and Structural Biology, Graduate Program in Biophysics, State University of New York at Stony Brook, Stony Brook, New York 11794-3400

Received March 9, 2007; Revised Manuscript Received July 18, 2007

ABSTRACT: Amyloid formation has been implicated in a wide range of human diseases including Alzheimer's disease, Parkinson's disease, and type 2 diabetes. In type 2 diabetes, islet amyloid polypeptide (IAPP, also known as amylin) forms cytotoxic amyloid deposits in the pancreas, and these are believed to contribute to the pathology of the disease. The mechanism of islet amyloid formation is not understood; however, recent proposals have invoked a role for incompletely processed proIAPP. In this model, incompletely processed proIAPP containing the N-terminal pro region is excreted and binds to heparan sulfate proteoglycans (HSPGs) of the basement membrane thereby establishing a high local concentration which can act as a seed for amyloid formation. Here we report biophysical proof-of-principle experiments designed to test the viability of this model. The model predicts that interactions with HSPGs should accelerate amyloid formation by the proIAPP processing intermediate, and this is indeed what is observed. Interaction with heparan sulfate leads to the rapid formation of an intermediate state with partial helical content which then converts, on a slower time scale, to amyloid fibrils. TEM shows that fibrils formed by the proIAPP processing intermediate in the presence and in the absence of heparan sulfate have the classic features of amyloid. Fibrils formed by the proIAPP processing intermediate are competent to seed amyloid formation by mature IAPP. The seeding experiments support a second major premise of the model, namely, that fibrils formed by the processing intermediate are capable of seeding amyloid formation by the mature peptide.

Amyloid deposition is a characteristic component of many human diseases, including Alzheimer's disease, Parkinson's disease, and type 2 diabetes (*1*, *2*). Human islet amyloid polypeptide (IAPP), also called amylin, is a 37 residue peptide that is responsible for pancreatic amyloid formation in type 2 diabetes (*3*−*7*). Synthetic amyloid fibrils are toxic to the insulin-producing β-cells, indicating that islet amyloid could contribute to the loss of β-cell mass and function in type 2 diabetes (*5*−*10*). The extent of amyloid deposition correlates with the severity of the disease, offering further evidence for a relationship between islet amyloid formation and type 2 diabetes (*10*). IAPP is synthesized in the pancreatic β-cells where it is stored with insulin in the insulin secretory granules (*11*). The normal physiological role of soluble IAPP is not entirely clear, but it is thought to act as an antagonist of insulin and is believed to play a role in gastric emptying, suppression of food intake, and glucose homeostasis (*12*−*16*).

The mechanism of islet amyloid formation is not well understood. IAPP secretion is coregulated with insulin secretion and is elevated in type 2 diabetes. However, overproduction of IAPP alone does not trigger amyloid formation, nor, with one exception, have mutations in the IAPP gene been implicated in islet amyloid formation (*5*, *17*). It has recently been proposed that defects in the processing of proIAPP[1] could play a critical role in triggering

† A.A. was supported in part by a GAANN fellowship from the Department of Education.

* Corresponding author: State University of New York at Stony Brook, Stony Brook, NY 11794-3400. Phone: (631) 632-9547. Fax: (631) 632-7960. E-mail: draleigh@notes.cc.sunysb.edu.

‡ Department of Chemistry.

§ Present address: Josin Diabetes Center, Harvard Medical School, One Joslin Place, Boston, MA 02215.

|| Graduate Program in Biochemistry and Structural Biology, Graduate Program in Biophysics.

[1] Abbreviations: CD, circular dichroism spectroscopy; DIPEA, *N*,*N*-diisopropylethylamine; DMF, *N*,*N*-dimethylformamide; DMSO, dimethyl sulfoxide; Fmoc, 9-fluorenylmethoxycarbonyl; GAG, glycosaminoglycan; HBTU, *O*-benzotriazol-1-yl-*N*,*N*,*N*′,*N*′-tetramethyluronium hexafluorophosphate; HFIP, hexafluoroisopropanol; HOBT, *N*-hydroxybenzotriazole monohydrate; HPLC, high performance liquid chromatography; HSPGs, heparan sulfate proteoglycans; IAPP, islet amyloid polypeptide; MALDI-TOF MS, matrix assisted laser desorption ionization-time of flight mass spectrometry; PAL-PEG, 5-(4′-Fmoc-aminomethyl-3′,5-dimethoxyphenyl) valeric acid; PC2, subtilisin-like prohormone convertase enzyme 2; PC(1/3), subtilisin-like prohormone convertase enzyme 1/3; proIAPP, pro-islet amyloid polypeptide; $proIAPP_{1-48}$, peptide corresponding to residues 1−48 of human pro-islet amyloid polypeptide; $proIAPP_{1-48}$/heparan sulfate, $proIAPP_{1-48}$ with heparan sulfate; $proIAPP_{1-48}$/dermatan sulfate, $proIAPP_{1-48}$ with dermatan sulfate; $proIAPP_{1-48}$/chondroitin sulfate, $proIAPP_{1-48}$ with chondroitin sulfate; TEM, transmission electron microscopy; TFA, trifluoroacetic acid.

10.1021/bi7004834 CCC: $37.00
Published on Web 10/09/2007

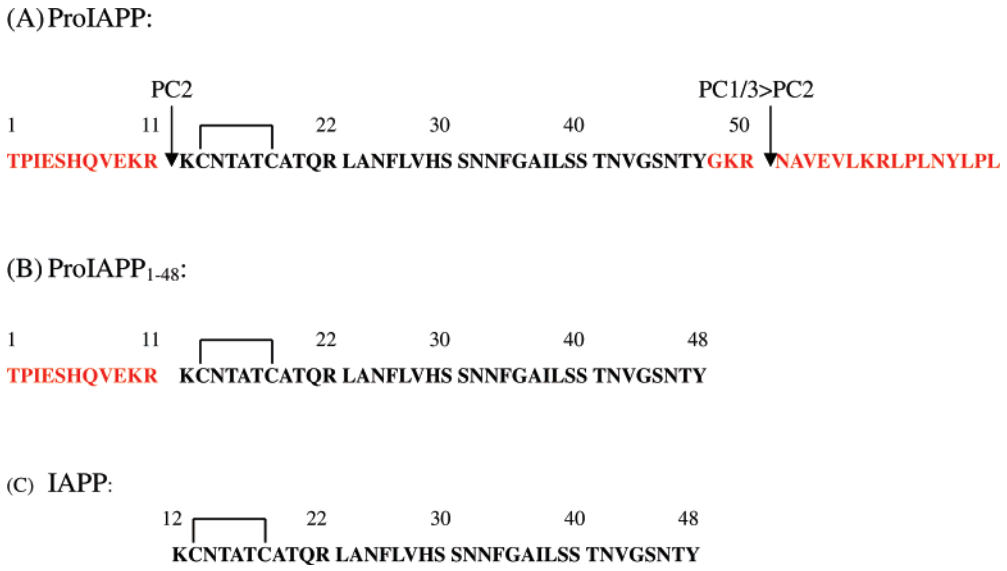

FIGURE 1: (A) The primary sequence of the 67 residue human proIAPP polypeptide. The N-terminal and C-terminal flanking regions of proIAPP are shown in red, and the black sequence corresponds to mature IAPP. Cleavage of proIAPP occurs at the two dibasic sites (Lys_{10}-Arg_{11}) and (Lys_{50}-Arg_{51}) indicated by the arrows. Further processing occurs at the C-terminus to yield amidated mature IAPP. (B) The primary sequence of the $proIAPP_{1-48}$ processing intermediate. (C) The primary sequence of mature IAPP. All three peptides have an intramolecular disulfide and an amidated C-terminus. The numbering system used corresponds to that of the complete pro sequence.

islet amyloid deposition (*18*−*22*). IAPP is initially synthesized as an 89 residue precursor (preproIAPP) (*11*). The signal sequence is removed proteolytically to produce the 67 residue pro hormone, proIAPP. ProIAPP is further processed to yield the mature 37 residue hormone. Post-translational processing of proIAPP occurs at two conserved dibasic sites and involves the same prohormone convertases that process proinsulin, PC(1/3) and PC2 (*21*−*24*). PC(1/3) is responsible for processing at the C-terminal dibasic site while PC2 favors cleavage at the N-terminal dibasic site (*23*−*26*). Normal processing of proIAPP is a two stage process that is initiated by cleavage at the C-terminal site in either the trans-Golgi network or secretory granule, while N-terminal cleavage occurs in the β-secretory granule. Additional posttranslational modifications include amidation of the C-terminus and formation of the intramolecular disulfide.

A portion of the secreted insulin is incompletely processed in type 2 diabetes, suggesting that the same could be true for IAPP. Immunohistochemical studies of islet amyloid have indicated the presence of the N-terminal region of proIAPP but not the C-terminal region, thus demonstrating the presence of a processing intermediate which contains the N-terminal prosequence (*27*, *28*). This intermediate corresponds to the first 48 residues of proIAPP and is designated $proIAPP_{1-48}$. Abnormal processing of proIAPP has been proposed to play an important role in islet amyloid formation and correlate with cell death (*19*, *20*, *22*). One hypothesis is that incorrectly processed proIAPP interacts with heparan sulfate proteoglycans (HSPGs) of the basement membrane (*18*). HSPGs are found in islet amyloid deposits and appear to be a general feature of amyloid plaques (*29*−*38*). The proteoglycan perlecan has been implicated in virtually all human amyloid diseases (*27*−*36*). HSPGs are ubiquitously expressed and have been proposed to serve as scaffolds for amyloid, stabilizing and possibly inducing amyloid formation. Peptide fragments derived from the N-terminal region of the $proIAPP_{1-48}$ processing intermediate have been shown to bind glycosaminoglycans (GAGs) (*18*, *20*), suggesting that

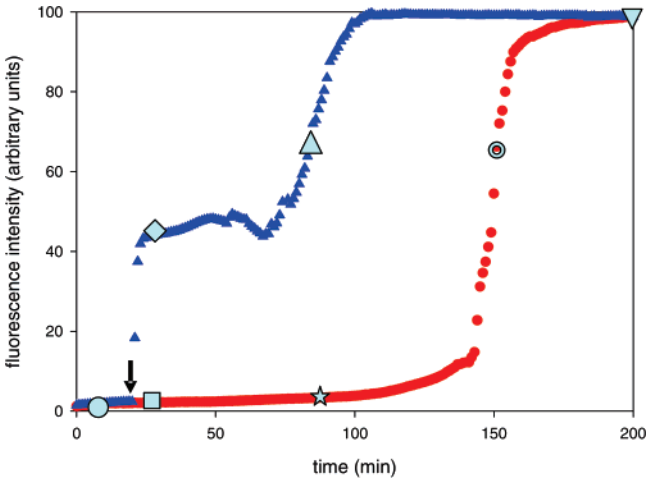

FIGURE 2: Effect of heparan sulfate upon amyloid formation by $proIAPP_{1-48}$. Heparan sulfate was added at 20 min as indicated by the arrow. The red curve corresponds to a solution of 32 μM $proIAPP_{1-48}$. The blue curve corresponds to a solution of 32 μM $proIAPP_{1-48}$ in the presence of 2.7 μM heparan sulfate (added at 20 min). The pH of the solutions was 7.4. The solutions contained 2% HFIP by volume and were continually stirred at 15 °C. The symbols indicate the time points at which CD spectra were recorded (Figure 3 and Figure 4).

interactions between HSPGs and $proIAPP_{1-48}$ might play a role in amyloid deposition in type 2 diabetes. In particular, Verchere and co-workers have proposed that improperly processed N-terminal extensions of proIAPP could bind to HSPGs upon secretion to the extracellular space and provide a seed for the formation of amyloid deposits *in vivo* (*18*). This model predicts that peptide GAG interactions should promote amyloid formation by the $proIAPP_{1-48}$ intermediate and also predicts that fibrils formed by the interaction of $proIAPP_{1-48}$ with GAGs should be competent to seed amyloid formation by mature IAPP. In this work, we report biophysical proof-of-principle studies of this proposal.

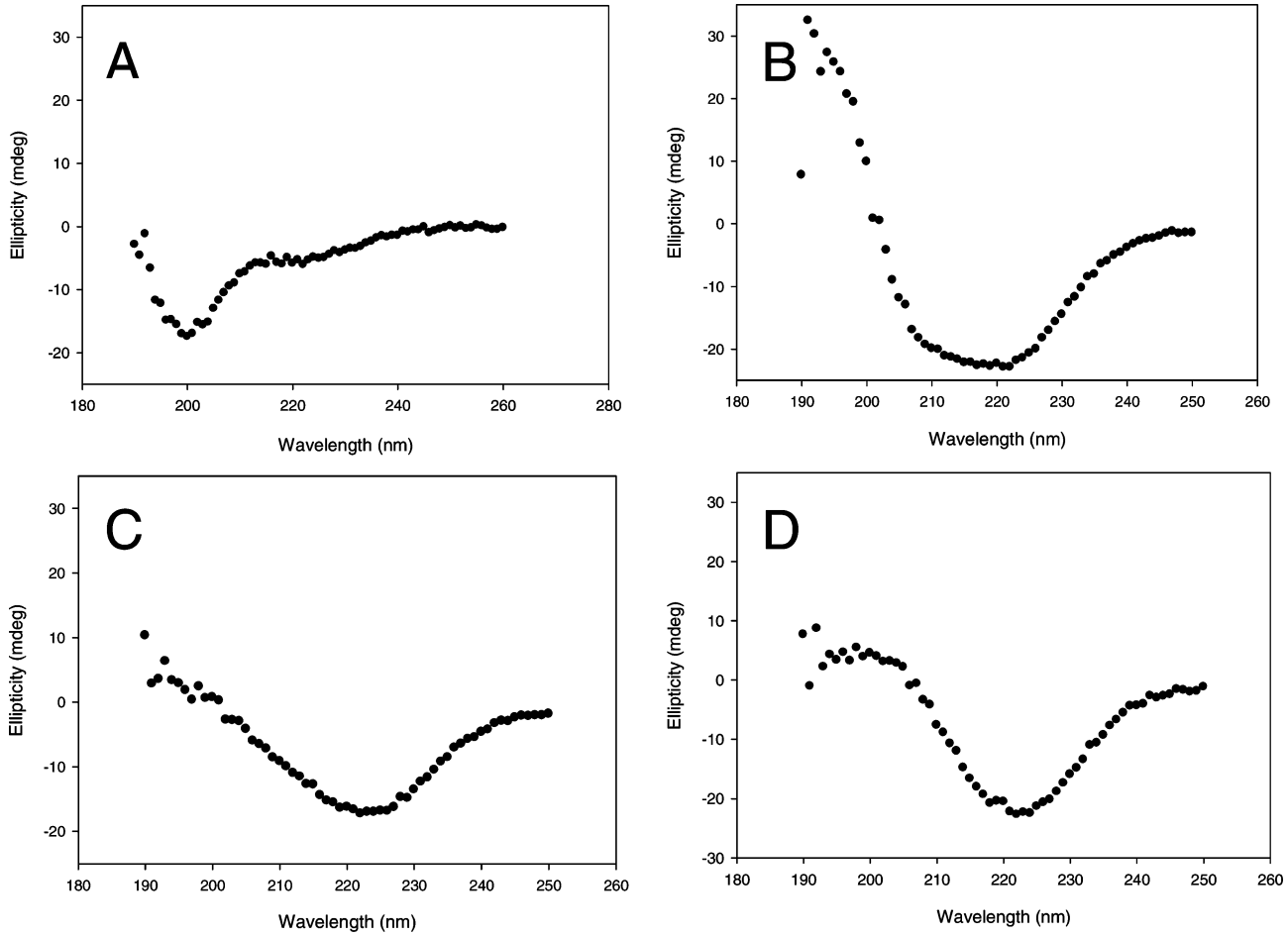

FIGURE 3: Far UV CD spectra of proIAPP$_{1-48}$ collected at four different time points after the initiation of the fibrilization reaction. Heparan sulfate was added at 20 min. The time points correspond to the times indicated in the kinetic trace displayed in Figure 2: (A) corresponds to the time point at 8 min (○), (B) corresponds to the time point at 24 min (◇), which corresponds to 4 min after the addition of heparan sulfate, (C) corresponds to the time point at 82 min (△), and (D) corresponds to the time point at the end of reaction at 200 min (▽). The sample used for the CD measurements was exactly the same as that used for the fluorescence experiment.

EXPERIMENTAL PROCEDURES

Peptide Synthesis and Purification. Peptides were synthesized on a 0.25 mmol scale using an applied Biosystems 433A peptide synthesizer, using 9-fluorenylmethoxycarbonyl (Fmoc) chemistry as described. Pseudoprolines were incorporated to facilitate the synthesis (*39*). The 5-(4′-Fmoc-aminomethyl-3′,5-dimethoxyphenol) valeric acid (PAL-PEG) resin was used to afford an amidated C-terminal. Standard Fmoc reaction cycles were used. The first residue attached to the resin, β-branched residues, residues directly following β-branched residues, and pseudoprolines were double coupled. Crude peptides were oxidized by dimethyl sulfoxide (DMSO) for 24 h at room temperature. The peptides were purified by reverse-phase HPLC using a Vydac C18 preparative column. Analytical HPLC was used to check the purity of the peptides before each experiment. The identity of the pure peptides was conformed by mass spectrometry using a Bruker MALDI-TOF MS (proIAPP$_{1-48}$, expected 5209.7, observed 5209.2; for IAPP, expected 3904.3, observed 3904.5).

Sample Preparation. A 1.58 mM peptide solution was prepared in 100% hexafluoroisopropanol (HFIP) and stored at −20 °C. Heparan sulfate, dermatan sulfate, and chondroitin sulfate were obtained from Sigma-Aldrich. 2 mg/2.2 mL GAG solutions were prepared by dissolving GAGs in 20 mM Tris-HCl buffer at pH 7.4. For the seeding experiments, preformed proIAPP/heparan sulfate seeds were produced by diluting 34 μL of filtered stock solution and 70 μL of heparan sulfate solution into 20 mM Tris-HCl buffer, which gave a final concentration of 32 μM proIAPP/38.2 μg/mL heparan sulfate in 2% HFIP. The solution was incubated with stirring for 80 min at 25 °C to obtain solutions of fibrils, which were used within 8 h for the seeding experiment.

Thioflavin-T Fluorescence. All fluorescence experiments were performed on a Jobin Yvon Horiba fluorescence spectrophotometer at an excitation wavelength of 450 nm and emission wavelength of 485 nm. The excitation and emission slits were set at 5 and 10 nm respectively. A 1.0 cm cuvette was used, and each point was averaged for 1 min. All solutions for these studies were prepared by diluting filtered stock solution (0.45 μm filter) into a Tris-HCl buffer (pH = 7.4) and thioflavin-T solution immediately before the measurement. The final concentration was 32 μM peptide and 32 μM thioflavin-T in 2% HFIP for all proIAPP$_{1-48}$/GAG experiments. The concentration of GAG was 38.2 μg/mL. The final concentrations of seeds used in proIAPP$_{1-48}$/heparan sulfate seeding experiments were 2.3 μg/mL heparan sulfate and 2 μM proIAPP in 2.2% HFIP. All solutions were stirred during the fluorescence experiments.

Circular Dichroism (CD). CD experiments were conducted with an Aviv model 62A DS circular dichroism spectrometer.

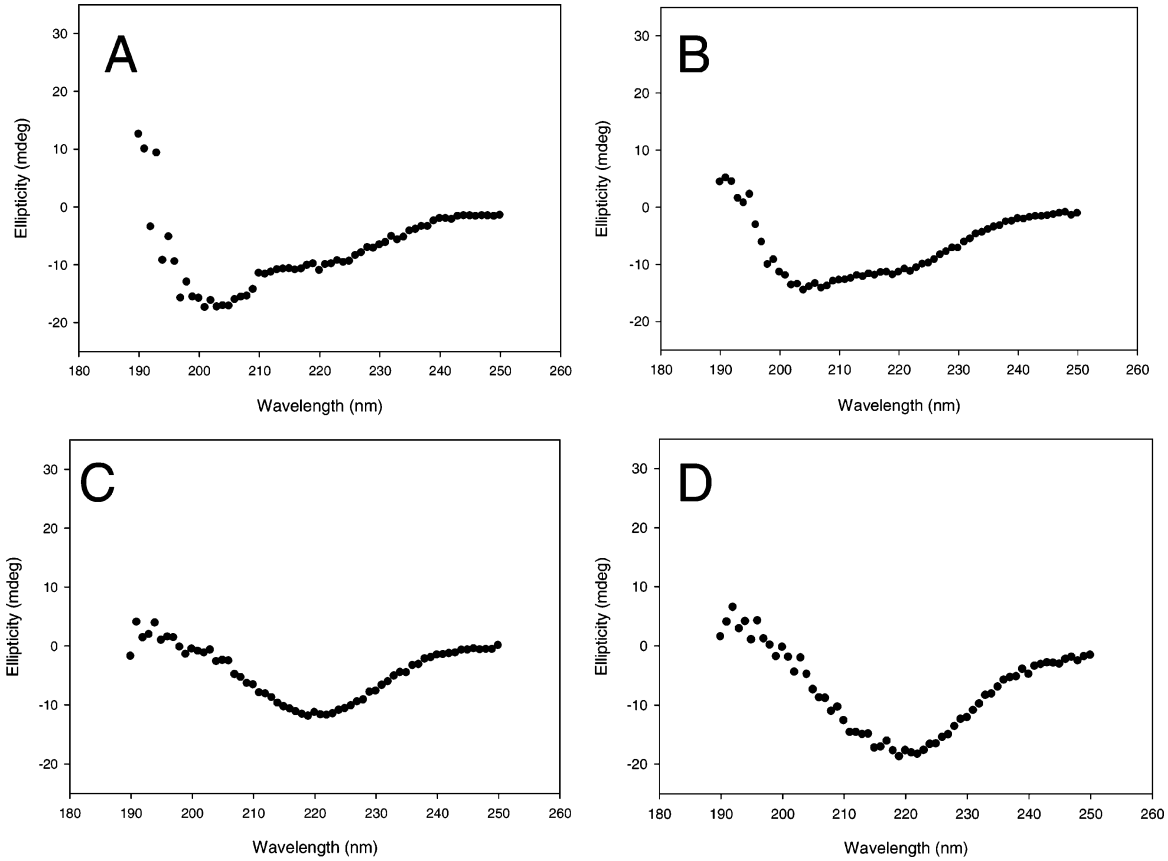

FIGURE 4: Far UV CD spectra of proIAPP$_{1-48}$ collected at four different time points after the initiation of the fibrilization reaction. No heparan sulfate was added. The time points correspond to the times indicated in the kinetic trace displayed in Figure 2: (A) corresponds to the time point at 24 min (□), (B) corresponds to the time point at 82 min (☆), (C) corresponds to the time point within the growth phase between 150 and 165 min (◎), and (D) corresponds to the time point at the end of reaction at 200 min (▽). The sample used for the CD measurements was exactly the same as that used for the fluorescence experiment.

CD experiments used exactly the same stock solutions as the thioflavin-T fluorescence measurements. The final concentration of peptide was 32 μM peptide. Some samples contained 38.2 μg/mL GAG. Spectra were recorded from 190 to 250 nm at 1 nm intervals in a 0.1 cm path length quartz cuvette at 15 °C.

Transmission Electron Microscopy (TEM). TEM was performed at Life Science Microscopy Center at the State University of New York at Stony Brook. Sample solutions for TEM were taken directly from thioflavin-T fluorescence assays. 15 μL of peptide solution was placed on a formvar 200 mesh copper grid and negatively stained with saturated uranyl acetate.

RESULTS AND DISCUSSION

Amyloid Formation by ProIAPP$_{1-48}$ Is Slower Than Wild Type but Is Accelerated by Heparan Sulfate. The sequences of proIAPP, the proIAPP$_{1-48}$ processing intermediate, and mature IAPP are shown in Figure 1. The locations of the prohormone cleavage sites are also indicated. The N-terminal extension of proIAPP$_{1-48}$ contains a pair of basic residues immediately adjacent to the first residue of the mature peptide; these basic residues are important for heparan sulfate binding (*18*, *20*). Fibril formation was initiated by diluting stock solutions of peptide, prepared in HFIP, into Tris-HCl buffer and then monitored by thioflavin-T fluorescence. Fluorescence detected thioflavin-T binding provides a convenient probe of the time course of fibril formation, since the quantum yield of the dye increases significantly upon binding to amyloid fibrils (*40*). The proIAPP processing intermediate, proIAPP$_{1-48}$, is capable of amyloid formation

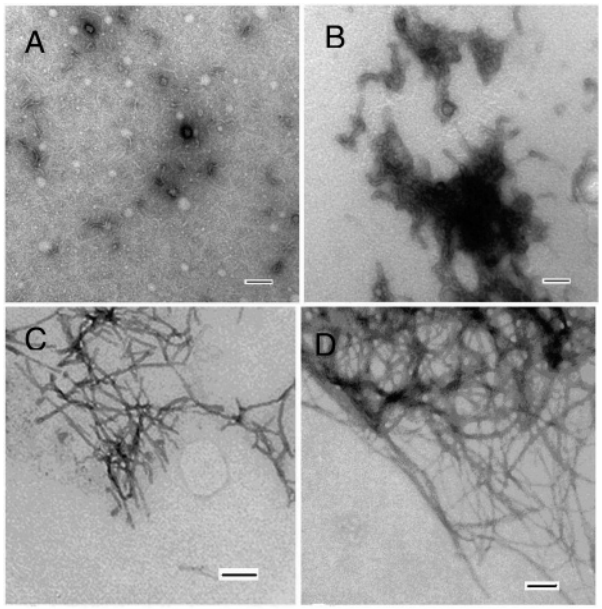

FIGURE 5: Transmission electron microscopy of proIAPP$_{1-48}$ aggregates formed in the presence and absence of heparan sulfate: (A) proIAPP$_{1-48}$ alone collected at 24 min, (B) proIAPP$_{1-48}$ plus heparan sulfate collected at 24 min, (C) proIAPP$_{1-48}$ alone collected after 200 min, (D) proIAPP$_{1-48}$ plus heparan sulfate collected after 200 min. Scale bars represent 100 nm.

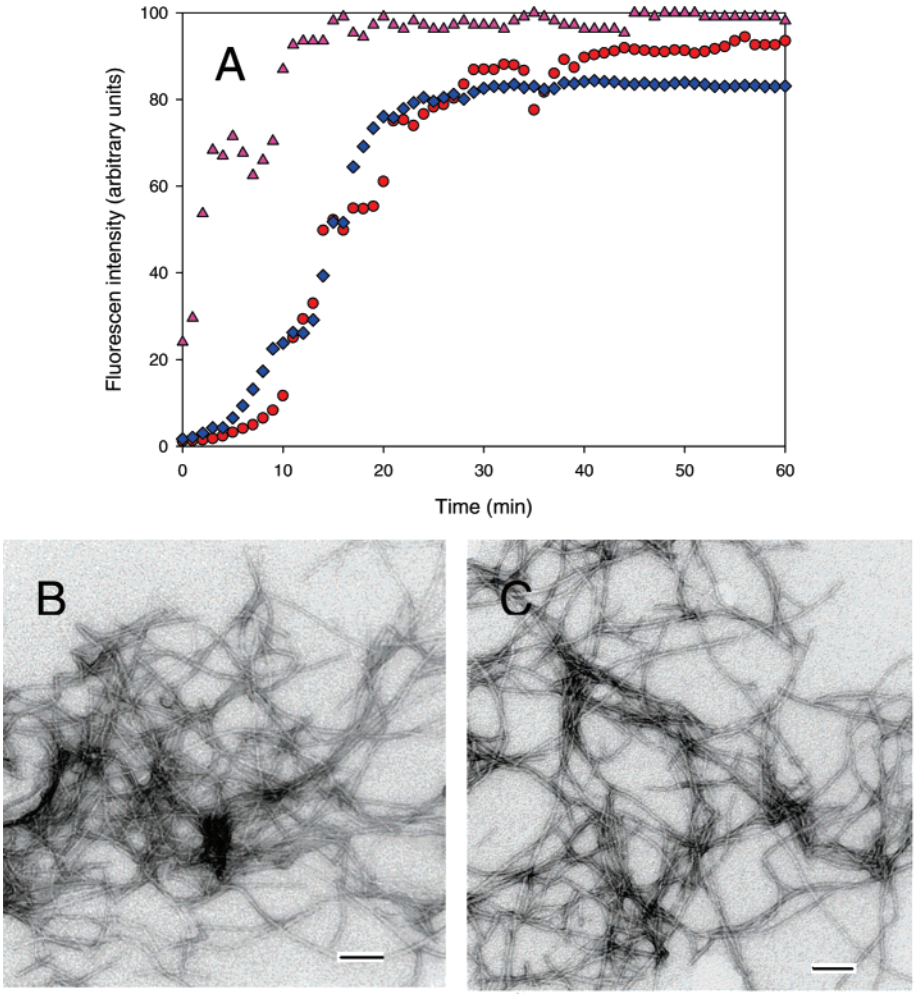

FIGURE 6: (A) Thioflavin-T monitored aggregation of mature IAPP and the effects of seeding: mature IAPP alone (●), mature IAPP with heparan sulfate added at time zero (◆), and mature IAPP seeded by proIAPP/heparan sulfate at time zero (▲). The seeds were added at 0 min. (B) TEM image of amyloid fibrils formed by mature IAPP in the absence of seeds. (C) TEM image of amyloid fibrils formed by mature IAPP in the presence of $proIAPP_{1-48}$/heparan sulfate seeds. Solutions used for TEM were identical to those used for the seeding studies. The pH of the solutions was 7.4. The solutions contained 2.2% HFIP by volume and were continually stirred at 25 °C. The scale bars in the TEM figures represent 100 nm.

in the absence of any added heparan sulfate, but it forms amyloid more slowly than mature IAPP with a lag phase 5- to 6-fold longer under the conditions of our studies (Figure 2). $ProIAPP_{1-48}$ has a lag phase on the order of 140 min under the conditions of these experiments while IAPP has a lag phase of 25 min. The slower rate of amyloid formation by $proIAPP_{1-48}$ is not surprising considering that the N-terminal extension is rich in polar and charged residues. Transmission electron microscopy (TEM) images of the end product of the reaction reveals that it consists of fibril material with dimensions typical of *in vitro* amyloid deposits.

We used the GAG heparan sulfate as a model for HSPG interactions since it has been previously employed in investigations of HSPG interactions with IAPP and proIAPP. The addition of heparan sulfate to a sample of $proIAPP_{1-48}$ accelerates amyloid formation (Figure 2). The results are quite interesting and somewhat surprising. Addition of heparan sulfate at 20 min after initiation of fibrillization led to a very rapid increase in thioflavin-T fluorescence, but the fluorescence intensity was less than that of wild type fibrils. The rapid initial rise was followed by an intermediate plateau and then a subsequent rapid growth phase which ultimately led to a final fluorescence similar to wild type. The final fluorescence intensity at the end of the reaction is essentially identical for the $proIAPP_{1-48}$ and $proIAPP_{1-48}$/heparan sulfate samples. The results are not an artifact caused by substoichiometric addition of heparan sulfate. Increasing the amount of heparan sulfate 3-fold leads to the same behavior (data not shown). The results are reproducible having been observed with several different samples. The unusual time course is not a consequence of waiting 20 min to add the heparan sulfate. Similar behavior is observed if the reaction is seeded at time zero. In that case, a rapid raise in fluorescence is once again observed leading to an intermediate plateau. The intermediate plateau persists for on the order of 30 min before a rapid increase to a final value that is similar to the level achieved by unseeded peptide (Supporting Information). The unusual multiphase reaction is not due to the choice of the cosolvent used to prepare the stock solutions since an intermediate plateau is also observed when DMSO, instead of HFIP, is used as the cosolvent (data not shown).

In order to follow the reaction in more detail, we collected CD spectra at the various time points indicated in Figure 2. For the $proIAPP_{1-48}$ plus heparan sulfate sample, the first spectrum was collected at 8 min, which corresponds to a time point prior to the addition of heparan sulfate. The

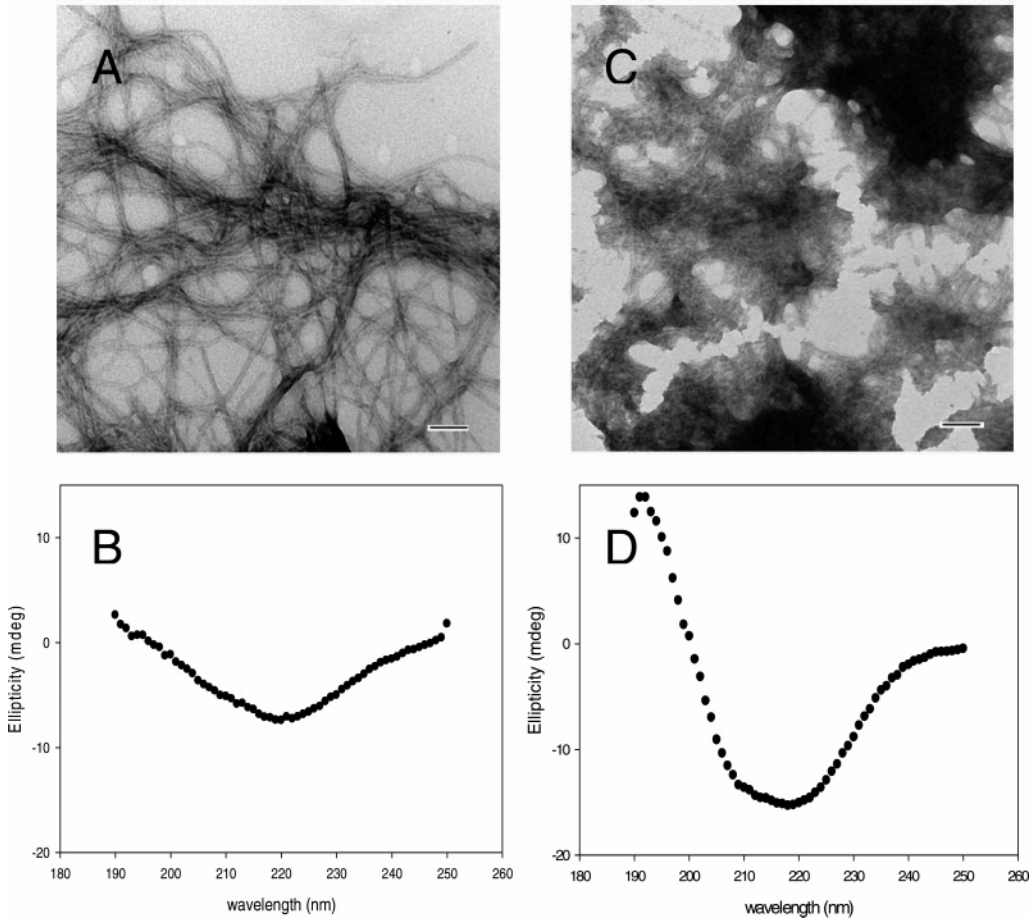

FIGURE 7: Comparison of the effects of the addition of chondroitin sulfate and dermatan sulfate to a solution of proIAPP$_{1-48}$: (A) TEM of the proIAPP$_{1-48}$/chondroitin sulfate sample after 200 min incubation, (B) CD spectrum of proIAPP$_{1-48}$/chondroitin sulfate sample after 200 min incubation, (C) TEM of the proIAPP$_{1-48}$/dermatan sulfate sample after 600 min incubation, and (D) CD spectrum of proIAPP$_{1-48}$/dermatan sulfate sample after 600 min incubation.

spectrum was similar to that expected for a largely unstructured peptide (Figure 3). Heparan sulfate was added at 20 min. The CD spectrum collected 4 min after the addition of heparan sulfate (total time 24 min) indicates a mixture of α-helix and β-sheet structure. The dramatic change in the CD spectrum confirms that binding to heparan sulfate causes a significant change in the conformational ensemble of proIAPP$_{1-48}$. Binding to heparan sulfate induces an intermediate which is partially helical. At 82 min, which corresponds to a time point in the second growth phase, the ensemble has converted into β-sheet rich structure. β-Sheet structure continues to develop, and the CD spectrum recorded at the end of the reaction (200 min) is typical of those observed for IAPP amyloid. It is natural to inquire whether conformational transitions observed after the addition of heparan sulfate are due to the binding of proIAPP$_{1-48}$ to heparan sulfate, or whether they are necessary steps in the amyloid formation pathway promoted by interactions with heparan sulfate. We collected CD spectra as a function of time for a sample of proIAPP$_{1-48}$ without any GAG in order to distinguish between these possibilities (Figure 4). The spectrum collected at 24 min is similar to the spectrum collected for the proIAPP$_{1-48}$ plus heparan sulfate prior to addition of GAG (i.e., the 8 min time point in Figure 3A). A spectrum collected during the lag phase of the proIAPP$_{1-48}$ sample (at 82 min) is consistent with the development of partial helical structure. A spectrum recorded in the growth

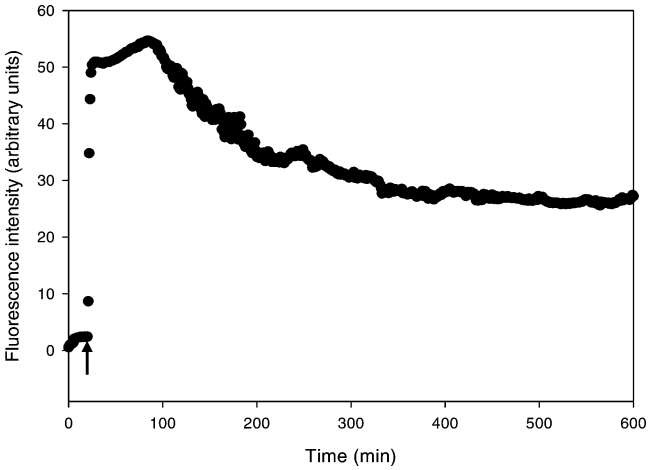

FIGURE 8: Effects of dermatan sulfate upon amyloid formation by proIAPP$_{1-48}$ as monitored by thioflavin-T fluorescence. Dermatan sulfate was added at 20 min as indicated by the arrow. The pH of the solutions was 7.4. The solutions contained 2% HFIP by volume and were continually stirred at 15 °C.

phase region of the reaction (Figure 4C) shows the conversion of the partially helical ensemble into β-sheet structures. The time dependent CD studies show that interactions with heparan sulfate are not required for the formation of the intermediate but do promote its rapid formation. CD, particularly of heterogeneous systems, is best viewed as a

semiqualitative technique, and we do not wish to imply that structural ensembles of the two samples are identical. TEM studies confirm that the addition of heparan sulfate induces significant changes and promotes aggregation. Aliquots from both samples were removed at 24 min, blotted onto TEM grids, and imaged (Figure 5). The sample of $proIAPP_{1-48}$ alone shows modest amounts of stained material but no obvious fibrils or large aggregates. The micrograph of the $proIAPP_{1-48}$ plus GAG sample is dramatically different, exhibiting dense mats of stained material. TEM images of the final products (200 min time point) confirm the presence of amyloid in both the $proIAPP_{1-48}$ sample and the $proIAPP_{1-48}$ plus heparan sulfate sample although there are some apparent minor differences (Figure 5). $ProIAPP_{1-48}$ formed long fibrils in the presence of heparan sulfate, while in the absence of heparan sulfate it formed a mixture of long fibrils and small short fibrils.

$ProIAPP_{1-48}$ Fibrils Can Seed Amyloid Formation by Wild Type IAPP. Having demonstrated that heparan sulfate can promote amyloid formation by the $proIAPP_{1-48}$ processing intermediate, we next sought to determine if these fibrils could efficiently seed fibril formation by fully processed wild type IAPP. It has been suggested that complexes formed by improperly processed $proIAPP_{1-48}$ and HSPGs could promote amyloid formation by mature IAPP (*18*). The data presented in Figure 6 demonstrates that the $proIAPP_{1-48}$/heparan sulfate fibrils are indeed capable of seeding amyloid formation by mature IAPP. Addition of the seeds to the reaction mixture abolished the lag phase (Figure 6). The effect is not simply due to interactions of mature IAPP with heparan sulfate since addition of heparan sulfate alone has only a very small effect upon the kinetics of amyloid formation by mature IAPP under these conditions. TEM measurements clearly demonstrate that amyloid is formed in both the seeded and unseeded reactions (Figure 6). The images of the amyloid formed by unseeded mature IAPP and by mature IAPP seeded with $proIAPP_{1-48}$/heparan sulfate fibrils are similar in appearance and have the classical amyloid morphology.

Demonstration of Specificity in $ProIAPP_{1-48}$ GAG Interactions. We examined the interaction of $proIAPP_{1-48}$ with two other GAGs in order to test if the interactions we observed with heparan sulfate are generic or if there is any specificity. Chondroitin sulfate and dermatan sulfate were used for these control studies. Chondroitin sulfate induced effects which were similar to those observed with heparan sulfate, namely, an initial rapid increase in thioflavin-T fluorescence followed by an intermediate plateau that led to a second rapid growth phase and then a final plateau. TEM images collected from this sample at the end of the reaction reveal the presence of extensive amyloid fibrils, while the CD spectrum is consistent with significant β-sheet structure (Figure 7). The situation is very different when dermatan sulfate is used. In this case, the rapid rise in thioflavin-T fluorescence is observed upon addition of the GAG, but the subsequent behavior is significantly different. There is a gradual decrease in thioflavin-T fluorescence leading to a final apparent steady-state value (Figure 8). We fail to observe the second growth phase that was detected with the two other GAGs even though the $proIAPP_{1-48}$/dermatan sulfate sample was followed for a significantly longer time (600 min vs 200 min) than the other samples. TEMs of the reaction mixture collected after the completion of the time course are very different from those of the $proIAPP_{1-48}$/heparan sulfate or $proIAPP_{1-48}$/chondroitin sulfate samples. A large amount of amorphous, densely stained material is present, but no fibrils are detected. The image is qualitatively similar to the one recorded of the $proIAPP_{1-48}$/heparan sulfate sample just after the addition of the GAG. CD spectra of this sample also differ significantly from the other GAG/$proIAPP_{1-48}$ samples; the spectrum appears noticeablely more helical (Figure 7).

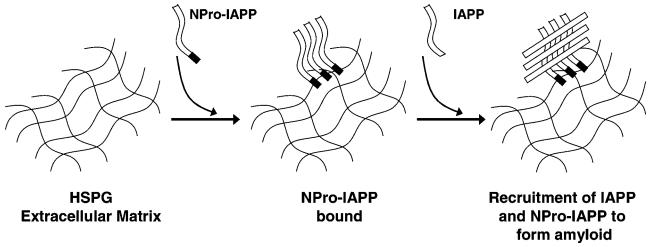

FIGURE 9: Schematic representation of how an increase in the production of incompletely processed IAPP (Npro-IAPP) could contribute to amyloid formation. Polypeptides with an uncleaved N-terminal extension (shaded) are able to bind to HSPGs in the extracellular matrix resulting in a high local concentration of peptide. This in turn could act as a seed for amyloid formation.

CONCLUSIONS

We have demonstrated that amyloid formation by the $proIAPP_{1-48}$ processing intermediate is promoted by its interaction with heparan sulfate. Heparan sulfate−peptide interactions likely enhance $proIAPP_{1-48}$ amyloid formation by promoting a high local concentration of the peptide. The GAG binding site has previously been shown to be located in the N-terminal half or two-thirds of the molecule (*18*, *20*). Binding to this region would leave the C-terminal region free to play a role in peptide self-association. The C-terminal portion of IAPP is very prone to aggregation and amyloid formation (*41*). Along these lines, it is interesting to note that a fragment composed of the first thirty residues of $proIAPP_{1-48}$, which lacks the C-terminal region, also interacts strongly with heparan sulfate but is far less prone to form amyloid in the presence of heparan sulfate (*20*).

The control experiments with chondroitin sulfate and dermatan sulfate demonstrate that the effects are not specific to heparan sulfate, but they also indicate that there is some specificity in the polypeptide GAG interaction. It is interesting that interactions with dermatan sulfate appear to trap the peptide in a state which is not able to undergo the final self-assembly into β-sheet fibrils, or at the very least slows it significantly. It may be that interactions with dermatan sulfate induce a conformation which is not competent to undergo the conversion to β-structure. Alternatively, the conformation of the peptide could be similar to that adopted in the presence of the other GAGs, but the interactions might be stronger with dermatan sulfate than with the other GAGs, and this might trap the intermediate. A detailed structure−function study will be required to sort out all of the details of $proIAPP_{1-48}$ GAG interactions. This is beyond the scope of the present study, but is clearly an interesting topic for further exploration.

One interesting feature of the seeding experiments is the observation of a partial helical intermediate. Although this may seem counterintuitive given that the final fibril structure is rich in β-sheet, there is a precedent for helical intermediates

in amyloid formation. Partial helical structure is induced when IAPP interacts with model vesicles and helical structure has been postulated to play a role in the membrane mediated association of IAPP (*42*−*43*). In addition, Teplow and co-workers have presented compelling evidence implicating an on pathway helical intermediate in Aβ amyloid formation (*44*−*45*).

Importantly, fibrils formed by proIAPP$_{1-48}$/heparan sulfate are competent to promote amyloid formation by mature IAPP. Models of islet amyloid formation that involve a critical role for interactions between proIAPP processing intermediates and the HSPG components of the extracellular matrix assume that such complexes can promote amyloid formation by mature IAPP (*18*). The work presented here provides the first direct evidence that this is indeed the case. Our observations provide *in vitro* proof-of-principle studies in support of the mechanism of amyloid formation initially proposed by Verchere and colleagues (*18*). A schematic diagram depicting the proposed mechanism is shown in Figure 9. ProIAPP$_{1-48}$ binds to HSPGs in the extracellular matrix leading to a high local concentration of aggregation prone peptide. This acts as a seed for further recruitment of proIAPP$_{1-48}$ and mature IAPP thus promoting amyloid formation.

Peptide and HSPG interactions are thought to play a general role in amyloidosis, and they may modulate cytotoxicity by mediating the interaction of amyloid fibrils with the cell membrane. Peptide HSPG interactions have been proposed as potential drug targets (*46*). There is an emerging view in the amyloid field that nonfibrillar oligomers or prefibrillar aggregates may be the toxic species in amyloid diseases. While the current study has not addressed the toxicity of the intermediate species observed, it is possible that conformational transitions induced in proIAPP$_{1-48}$ by interactions with GAGs could result in more toxic aggregates. The work reported here demonstrates the importance of interactions between proIAPP processing intermediates and GAGs, at least *in vitro*, suggesting that targeting proIAPP HSPG interactions may be an interesting strategy (*47*).

ACKNOWLEDGMENT

We thank Ms. Ruchi Gupta for helpful discussions and experimental assistance.

SUPPORTING INFORMATION AVAILABLE

One figure showing the effect of the addition of heparan sulfate at time equal zero on the kinetics of amyloid formation by proIAPP$_{1-48}$. This material is available free of charge via the Internet at http://pubs.acs.org.

REFERENCES

1. Sipe, J. D. (1994) Amyloidosis, *Crit. Rev. Clin. Lab. Sci. 31*, 325−354.
2. Vendruscolo, M., Zurdo, J., Macphee, C. E., Dobson, C. M. (2003) Protein folding and misfolding: A paradigm of self-assembly and regulation in complex biological systems, *Philos. Trans. R. Soc. London, Ser. A: Math., Phys. Eng. Sci. 361*, 1205−1222.
3. Westermark, P., Wernstedt, C., Wilander, E., Hayden, D. W., O'Brien, T. D., and Johnson, K. H. (1987) Amyloid fibrils in human insulinoma and islets of Langerhans of the diabetic cat are derived from a neuropeptide-like protein also present in normal islet cells, *Proc. Natl. Acad. Sci. U.S.A. 84*, 3881−3885.
4. Cooper, G. J. S., Willis, A. C., Clark, A., Turner, R. C., Sim, R. B., and Reid, K. B. M. (1987) Purification and characterization of a peptide from amyloid-rich pancreases of type 2 diabetic patients, *Proc. Natl. Acad. Sci. U.S.A. 84*, 8628−8632.
5. Kahn, S. E., Andrikopoulos, S., and Verchere, C. B. (1999) Islet amyloid: a long recognized but underappreciated pathological feature of type 2 diabetes, *Diabetes 48*, 241−246.
6. Clark, A., Lewis, C. E., Willis, A. C., Cooper, G. J. S., Morris, J. F., Reid, K. B. M., and Turner, R. C. (1987) Islet amyloid formed from diabetes-associated peptide may be pathogenic in type-2 diabetes, *Lancet 2*, 231−234.
7. Hull, R. L., Westermark, G. T., Westermark, P., and Kahn, S. E. (2004) Islet amyloid: a critical entity in the pathogenesis of type 2 diabetes, *J. Clin. Endocrinol. Metab. 89*, 3629−3643.
8. Butler, A. E., Janson, J., Bonner-Weir, S., Ritzel, R., Rizza, R. A., and Butler, P. C. (2003) β-Cell deficit and increased β-cell apoptosis in humans with type 2 diabetes, *Diabetes 52*, 102−110.
9. Clark, A., Wells, C. A., Buley, I. D., Cruickshank, J. K., Vanhegan, R. I., Matthews, D. R., Cooper, G. J. S., Holman, R. R., and Turner, R. C. (1988) Islet amyloid, increased α-cells, reduced β-cells and exocrine fibrosis: quantitative changes in the pancreas in type 2 diabetes, *Diabetes Res. Clin. Pract. 9*, 151−159.
10. Rocken, C., Linke, R. P., and Saeger, W. (1992) Immunohistology of islet amyloid polypeptide in diabetes mellitus: semiquantitative studies in a post-mortem series, *Virchows Arch. A: Pathol. Anat. Histopathol. 421*, 339−344.
11. Sanke, T., Bell, G. I., Sample, C., Rubenstein, A. H., and Steiner, D. F. (1988) An islet amyloid peptide is derived from an 89-amino acid precursor by proteolytic processing, *J. Biol. Chem. 263*, 17243−17246.
12. Rushing, P. A., Hagan, M. M., Seeley, R. J., Lutz, T. A., D'Alessio, D. A., Air, E. L., and Woods, S. C. (2001) Inhibition of central amylin signaling increases food intake and body adiposity in rats, *Endocrinology 142*, 5035−5038.
13. Clementi, G., Caruso, A., Cutuli, V. M. C., de bernardis, E., Prato, A., and Amico-Roxas, M. (1996) Amylin given by central or peripheral routes decreases gastric emptying and intestinal transit in the rat, *Experientia 52*, 677−679.
14. Leighton, B., and Cooper, G. J. S. (1988) Pancreatic amylin and calcitonin gene-related peptide cause resistance to insulin in skeletal-muscle *in vitro*, *Nature 335*, 632−635.
15. Ohsawa, H., Kanatsuka, A., Yamaguchi, T., Makino, H., and Yoshida, S. (1989) Islet amyloid polypeptide inhibits glucose-stimulated insulin secretion from isolated rat pancreatic islets, *Biochem. Biophys. Res. Commun. 160*, 961−967.
16. Akesson, B., Panagiotidis, G., Westermark, P., and Lundquist, I. (2003) Islet amyloid polypeptide inhibits glucagon release and exerts a dual action on insulin release from isolated islets, *Regul. Pept. 111*, 55−60.
17. Cooper, G. J. S. (1994) Amylin compared with calcitonin gene-related peptide: structure, biology, and relevance to metabolic disease, *Endocr. Rev. 15*, 163−201.
18. Park, K., and Verchere, C. B. (2001) Identification of a heparin binding domain in the N-terminal cleavage site of pro-islet amyloid polypeptide. Implications for islet amyloid formation, *J. Biol. Chem. 276*, 16611−16616.
19. Paulsson, J. F., and Westermark, G. T. (2005) Aberrant processing of human proislet amyloid polypeptide results in increased amyloid formation, *Diabetes 54*, 2117−2125.
20. Abedini, A., Tracz, S. M., Cho, J. H., and Raleigh, D. P. (2006) Characterization of the heparin binding site In the N-Terminus of human pro-Islet amyloid polypeptide: Implications for amyloid formation, *Biochemistry 45*, 9228−9237.
21. Marzban, L., Rhodes, C. J., Steiner, D. F., Haataja, L., Halban, P. A., and Verchere, C. B. (2006) Impaired NH2-terminal processing of human proislet amyloid polypeptide by the prohormone convertase PC2 leads to amyloid formation and cell death, *Diabetes 55*, 2192−2201.
22. Paulsson, J. F., Andersson, A., Westermark, P., and Westermark, G. T. (2006) Intracellular amyloid-like deposits contain unprocessed pro-islet amyloid polypeptide (proIAPP) in beta cells of transgenic mice overexpressing the gene for human IAPP and transplanted human islets, *Diabetologia 49*, 1237−1246.
23. Marcinkiewicz, M., Ramla, D., Seidah, N. G., and Chretien, M. (1994) Developmental expression of the prohormone convertases PC1 and PC2 in mouse pancreatic islets, *Endocrinology 135*, 1651−1660.

24. Furuta, M., Yano, H., Zhou, A., Rouille, Y., Holst, J. J., Carroll, R., Ravazzola, M., Orci, L., Furuta, H., and Steiner, D. F. (1997) Defective prohormone processing and altered pancreatic islet morphology in mice lacking active SPC2, *Proc. Natl. Acad. Sci. U.S.A. 94*, 6646−6651.
25. Wang, J., Xu, J., Finnerty, J., Furuta, M., Steiner, D. F., and Verchere, C. B. (2001) The prohormone convertase enzyme 2 (PC2) is essential for processing proislet amyloid polypeptide at the NH_2-terminal cleavage site, *Diabetes 50*, 534−539.
26. Marzban, L., Trigo-Gonzalez, G., Zhu, X., Rhodes, C. J., Halban, P. A., Steiner, D. F., and Verchere, C. B. (2004) Role of β-cell prohormone convertase PC (1/3) in processing of pro-islet amyloid polypeptide, *Diabetes 53*, 141−148.
27. Westermark, G. T., Steiner, D. F., Gebre-Medhin, S., Engstrom, U., and Westermark, P. (2000) Proislet amyloid polypeptide immunoreactivity in the islets of Langerhans, *Upsala J. Med. Sci. 105*, 97−106.
28. Westermark, P., Engström, U., Westermark, G. T., Johnson, K. H., Permerth, J., and Betsholtz, C. (1989) Islet amyloid polypeptide (IAPP) and pro-IAPP immunoreactivity in human islets of Langerhans, *Diabetes Res. Clin. Pract. 7*, 219−226.
29. Young, I. D., Ailles, L., Narindrasorasak, S., Tan, R., and Kisilevsky, R. (1992) Localization of the basement membrane heparan sulfate proteoglycans in islet amyloid deposits in type 2 diabetes mellitus, *Arch. Pathol. Lab. Med. 116*, 951−954.
30. Watson, D. J., Lander, A. D., and Selkoe, D. J. (1997) Heparin-binding properties of the amyloidogenic peptides Aβ and amylin. Dependence on aggregation state and inhibition by Congo Red, *J. Biol. Chem. 272*, 31617−31624.
31. Castillo, G. M., Cummings, J., Yang, W., Judge, M. E., Sheardown, M. J., Rimvall, K., Hansen, J. B., and Snow, A. D. (1998) Sulfate content and specific glycosaminoglycan backbone of perlecan are critical for perlecan's enhancement of islet amyloid polypeptide (amylin) fibril formation, *Diabetes 47*, 612−620.
32. Snow, A. D., and Wight, T. N. (1989) Proteoglycans in the pathogenesis of Alzheimer's disease and other amyloidosis, *Neurobiol. Aging 10*, 481−497.
33. Castillo, G. M., Ngo, C., Cummings, J., Wight, T. N., and Snow, A. D. (1997) Perlecan binds to the β-amyloid proteins (Aβ) of Alzheimer's disease, accelerates Aβ fibril formation, and maintains Aβ fibril stability, *J. Neurochem. 69*, 2452−2465.
34. Inoue, S. (2001) Basement membrane and β amyloid fibrillogenesis in Alzheimer's disease, *Int. Rev. Cytol. 210*, 121−161.
35. Ancsin, J. B. (2003) Amyloidogenesis: historical and modern observations point to heparan sulfate proteoglycans as a major culprit, *Amyloid: J. Protein Folding Disord. 10*, 67−79.
36. Potter-Perigo, S., Hull, R. L., Tsoi, C., Braun, K. R., Andrikopoulos, S., Teague, J., Verchere, C. B., Kahn, S. E., and Wright, T. N. (2003) Proteoglycans synthesized and secreted by pancreatic islet β-cells bind amylin, *Arch. Biochem. Biophys. 413*, 182−190.
37. Yamamoto, S., Yamaguchi, I., Hasegawa, K., Tsutsumi, S., Goto, Y., Gejyo, F., and Naiki, H. (2004) Glycosaminoglycans enhance the trifluoroethanol-induced extension of β_2-microglobulin-related amyloid fibrils at a neutral pH, *J. Am. Soc. Nephrol. 15*, 126−133.
38. Suk, J. Y., Zhang, F., Balch, W. E., Linhardt, R. J., and Kelly, J. W. (2006) Heparin accelerates gelsolin amyloidogenesis, *Biochemistry 45*, 2234−2242.
39. Abedini, A., and Raleigh, D. P. (2005) Incorporation of pseudoproline derivatives allows the facile synthesis of human IAPP, a highly amyloidogenic and aggregation-prone polypeptide, *Org. Lett. 7*, 693−696.
40. LeVine, H. (1995) Thiofalvin T interactions with amyloid β-sheet structures, *Amyloid: Int. J. Exp. Clin. Invest. 2*, 1−6.
41. Nilsson, M. R., and Raleigh, D. P. (1999) Analysis of amylin cleavage products provides new insights into the amyloidogenic region of human amylin, *J. Mol. Biol. 294*, 1375−1385.
42. Knight, J. D., Hebda, J. A., and Miranker, A. D. (2006) Conserved and cooperative assembly of membrane-bound alpha-helical states of islet amyloid polypeptide, *Biochemistry 45*, 9496−9508.
43. Jayasinghe, S. A., and Laugen, R. (2005) Lipid membranes modulate the structure of islet amyloid polypeptide, *Biochemistry 44*, 12113−12119.
44. Kirkitadze, M. D., Condron, M. M., and Teplow, D. B. (2001) Identification and characterization of key kinetic intermediates in amyloid β-protein fibrillogenesis, *J. Mol. Biol. 312*, 1103−1119.
45. Teplow, D. B., Lazo, N. D., Bitan, G., Bernstein, S., Wyttenbach, T., Bowers, M. T., Baumketner, A., Shea, J. E., Urbanc, B., Cruz, L., Borreguero, J., and Stanley, H. E. (2006) Elucidating amyloid β-protein folding and assembly: A multidisciplinary approach, *Acc. Chem. Res. 39*, 635−645.
46. Elimova, E., Kisilevsky, R., Szarek, W. A., and Ancsin, J. B. (2004) Amyloidogenesis recapitulated in cell culture: a peptide inhibitor provides direct evidence for the role of heparan sulfate and suggests a new treatment strategy, *FASEB J. 18*, 1749−1751.
47. Conde-Knape, K. (2001) Heparan sulfate proteoglycans in experimental model of diabetes: a role for perlecan in diabetes complications, *Diabetes Metab. Res. Rev. 17*, 412−421.

BI7004834